Development/Plasticity/Repair

# Silencing the SPCA1 (Secretory Pathway $Ca^{2+}$-ATPase Isoform 1) Impairs $Ca^{2+}$ Homeostasis in the Golgi and Disturbs Neural Polarity

**M. Rosario Sepúlveda,[1,2] Jo Vanoevelen,[1] Luc Raeymaekers,[1] Ana M. Mata,[2] and Frank Wuytack[1]**

[1]Laboratory of $Ca^{2+}$-transport ATPases, Department of Molecular Cell Biology, Faculty of Medicine, Catholic University of Leuven, B-3000 Leuven, Belgium, and [2]Departamento de Bioquímica y Biología Molecular y Genética, Facultad de Ciencias, Universidad de Extremadura, 06071 Badajoz, Spain

**Neural cell differentiation involves a complex regulatory signal transduction network in which $Ca^{2+}$ ions and the secretory pathway play pivotal roles. The secretory pathway $Ca^{2+}$-ATPase isoform 1 (SPCA1) is found in the Golgi apparatus where it is actively involved in the transport of $Ca^{2+}$ or $Mn^{2+}$ from the cytosol to the Golgi lumen. Its expression during brain development in different types of neurons has been documented recently, which raises the possibility that SPCA1 contributes to neuronal differentiation. In the present study, we investigated the potential impact of SPCA1 on neuronal polarization both in a cell line and in primary neuronal culture. In N2a neuroblastoma cells, SPCA1 was immunocytochemically localized in the juxtanuclear Golgi. Knockdown of SPCA1 by RNA interference markedly delayed the differentiation in these cells. The cells retarded in differentiation showed increased numbers of neurites of reduced length compared with control cells. $Ca^{2+}$ imaging assays showed that the lack of SPCA1 impaired Golgi $Ca^{2+}$ homeostasis and resulted in disturbed trafficking of different classes of proteins including normally Golgi-localized cameleon GT-YC3.3, bearing a Golgi-specific galactosyltransferase N terminus, and a normally plasma membrane-targeted, glycosyl phosphatidyl inositol-anchored cyan fluorescent protein construct. Also in hippocampal primary neurons, which showed a differential distribution of SPCA1 expression in Golgi stacks depending on differentiation stage, partial silencing of SPCA1 resulted in delayed differentiation, whereas total suppression drastically affected the cell survival. The disturbed overall cellular $Ca^{2+}$ homeostasis and/or the altered targeting of organellar proteins under conditions of SPCA1 knockdown highlight the importance of SPCA1 function for normal neural differentiation.**

## Introduction

Neurons are one of the most morphologically complex, distinctly polarized cells with a high degree of membrane specialization, comprising a well developed complex of organelles belonging to the secretory pathway. The Golgi and other elements of the secretory pathway are involved in membrane addition and in the differential targeting of plasma membrane proteins to the correct plasma membrane subdomains in these polarized cells. As such, it takes a pivotal position for various neural polarized functions such as synaptic transmission and plasticity (Tang, 2001; Sytnyk et al., 2004). Recent studies highlight the central role of Golgi-localized proteins in controlling neural development and polarity (Horton et al., 2005; Ye et al., 2007; Chua and Tang, 2008; Yin et al., 2008). In the secretory pathway, both $Ca^{2+}$ and $Mn^{2+}$ ions act as important cofactors or regulators of many cellular activities including signaling cascades and the processing and trafficking of proteins and membranes. Therefore, the maintenance of optimal concentrations of these ions is very important for the membrane specialization of neurons.

The secretory pathway $Ca^{2+}$-ATPases (SPCA1, 2) are found in the membranes of the Golgi apparatus and constitute the most recently identified P-type $Ca^{2+}$ pumps in neural tissue, where SPCA1 is the major isoform (Wootton et al., 2004; Vanoevelen et al., 2005; Xiang et al., 2005; Murin et al., 2006; Sepúlveda et al., 2007). Together with $Ca^{2+}$-ATPases of the plasma membrane (PMCA) and of the sarco(endo)plasmic reticulum (SERCA), SPCAs are active participants in neural $Ca^{2+}$ homeostasis (Wootton et al., 2004; Mata and Sepúlveda, 2005; Sepúlveda et al., 2007). SPCAs also play a key task in $Mn^{2+}$ homeostasis, since they are the only known P-type ATPases that can transport $Mn^{2+}$ with high affinity (Van Baelen et al., 2001; Ton et al., 2002). In a previous work, we have shown the presence of SPCA1 in the soma and in the proximal part of dendritic trunks of main brain neurons from the earliest postnatal stages on (Sepúlveda et al., 2008). However, the contribution of SPCA1 to these developmental processes remained unknown. Such a role is suggested by the fact that an SPCA1 knock-out mouse presents a disturbed

Received April 29, 2009; accepted Aug. 1, 2009.

This work was supported by Fonds voor Wetenschappelijk Onderzoek (FWO)-Vlaanderen, Belgium Grant G.0646.08; Interuniversity Attraction Poles Programme Belgian Science Policy P6/28 (F.W.); Ministerio de Educación y Ciencia, Spain Grant BFU2008-00182; and the Fundación Marcelino Botín (A.M.M.) M.R.S. received a postdoctoral fellowship from Katholieke Universiteit Leuven (K.U.Leuven), Belgium, and a fellowship from Programa de Reincorporación de Doctores, Junta de Extremadura, Spain. J.V. was a Postdoctoral Fellow of the FWO. We thank Dr. P. Vangheluwe for helpful discussions and E. Larivière and Szilvia Baron for technical support. We thank Dr. W. Annaert [Katholieke Universiteit Leuven (K.U.Leuven)] for the first test in hippocampal culture and Dr. F. van Leuven, A. Kremer, and P. Borghgraef (K.U.Leuven) for help with the preparation of the primary hippocampal cultures.

Correspondence should be addressed to Dr. Frank Wuytack, Laboratory of $Ca^{2+}$-transport ATPases, Department of Molecular Cell Biology, Faculty of Medicine, Katholieke Universiteit Leuven, B-3000 Leuven, Belgium. E-mail: Frank.Wuytack@med.kuleuven.be.

J. Vanoevelen's present address: Hubrecht Institute for Developmental Biology and Stem Cell Research, 3584 CT Utrecht, The Netherlands.

DOI:10.1523/JNEUROSCI.2014-09.2009

 0270-6474/09/2912174-09$15.00/0

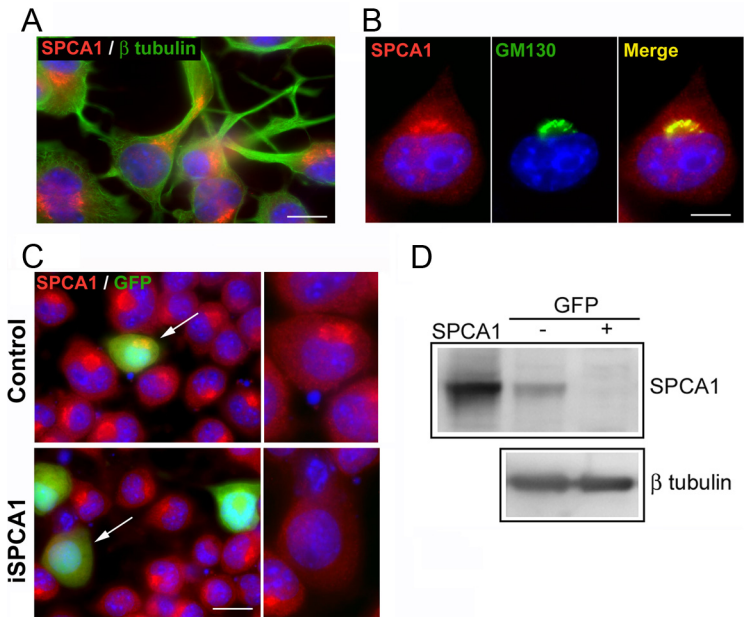


**Figure 1.** Endogenous localization of SPCA1 in differentiated N2a cells and SPCA1 knockdown. ***A***, Double immunofluorescence staining of SPCA1 (red) and $\beta$ tubulin (green) to visualize neurites generated after differentiation with retinoic acid. DAPI staining (blue) was used to visualize the cellular nuclei. ***B***, Colocalization of SPCA1 (red) and the Golgi-marker GM130 (green). ***C***, N2a cells transfected with pSUPER empty vector (control) and with pSUPER-mouseSPCA1 (iSPCA1), showing the silencing of SPCA1 expression by immunofluorescence staining with anti-SPCA1 (red). Insets, GFP positive-transfected cells (green; arrows) are shown for SPCA1 expression. ***D***, Western blot (10 $\mu$g of protein/lane) of iSPCA1-transfected N2a cells after sorting by FACS of the GFP− and GFP+ cells. hSPCA1 overexpressed in COS cells (0.1 $\mu$g) was used as the control (SPCA1), and $\beta$ tubulin immunoreaction was used as the loading control. SPCA1 expression relative to $\beta$ tubulin assessed from the integrated density of the corresponding bands decreased significantly from 1.0 $\pm$ 0.04 arbitrary units (a.u.) in the GFP− cells to 0.09 $\pm$ 0.03 a.u. in the GFP+ cells. Data are mean $\pm$ SE from two assays ( $p \leq 0.05$). Scale bars: ***A***, 20 $\mu$m; ***B***, 13 $\mu$m; ***C***, 38 $\mu$m.

neural tube development and Golgi stress (Okunade et al., 2007). To further explore the role of SPCA1 during development, in this study we have determined the localization of SPCA1 in the Neuro2a (N2a) neuroblastoma cell line and in primary neural cultures. We explored the effect of SPCA1 suppression by interference RNA on the generation, number, and dimensions of the neurites and assessed the functional impact of the intervention on $Ca^{2+}$ homeostasis. The results report a clear involvement of the SPCA1 pump in differentiation and in establishing polarity in neural cells.

## Materials and Methods

*Materials.* Retinoic acid, thapsigargin, and ionomycin were from Sigma. Fura-2AM was from Invitrogen. The polyclonal rabbit anti-SPCA1 (Van Baelen et al., 2003) and anti-SERCA2b (Wuytack et al., 1989) antibodies were described previously. The anti-$\beta$ tubulin monoclonal antibody was from Sigma, and the GM130 monoclonal antibody was from BD Biosciences. The SM132 monoclonal antibody was a gift from Dr. F. van Leuven (Katholieke Universiteit Leuven), the cDNA of the Golgi-cameleon GT-YC3.3 (Griesbeck et al., 2001) was provided by Dr. R. Tsien (University of California, San Diego, La Jolla, CA), and CFP-GL-GPI [i.e., a glycosyl phosphatidyl inositol (GPI)-anchored protein containing a consensus *N*-glycosylation site (GL) (Keller et al., 2001)] was provided by Dr. N. M. Hooper (University of Leeds, Leeds, UK). All other reagents were of the highest purity available.

*Construction of pSUPER-mouseSPCA1 RNAi vector.* To suppress the mouse SPCA1 transcripts, we constructed a pSUPER-mouseSPCA1 vector following the protocol described by Van Baelen et al. (2003). The pSUPER vector was provided by Dr. R. Agami (The Netherlands Cancer Institute, Amsterdam, The Netherlands). The 19 nt sequence derived from the mouse SPCA1 target transcript was 5′-GTGATCGTTGATGGTGATG-3′ and corresponds to nucleotides 1537-1555 of the mouse SPCA1 coding sequence (accession number NM_175025).

*N2a cell culture and DNA transfection.* N2a cells were cultured in growth medium constituted by DMEM/Ham F-12 medium containing 10% fetal calf serum (FCS) and supplemented with 100 U/ml penicillin, 100 U/ml streptomycin, 1 mM L-glutamine, and 1 mM sodium pyruvate. Cells were seeded on gelatin-coated glass coverslips or in chamber slides at a density of 10,000 cells/slide. Transfection of pSUPER-mouseSPCA1 was performed with GenJuice transfection reagent (Merck). Cells were cotransfected with green fluorescent protein (GFP) to identify transfected cells, in a ratio of 13-fold molar excess of the pSUPER-mouseSPCA1, so that it can be assumed that GFP-positive cells were also transfected successfully with pSUPER-SPCA1. After incubation for 60 h at 37°C in a humidified environment of 5% $CO_2$–95% air, differentiation of cells was induced with 20 $\mu$M retinoic acid in medium with 2% FCS.

*Sorting of GFP-positive cells.* Fluorescence-activated cell sorting (FACS) was done by using the FACS Vantage SE sorter (BD Biosciences). Afterward, cells were lysed in 25 mM HEPES/KOH, pH 7.5, 0.3 mM NaCl, 1.5 mM $MgCl_2$, 0.5 mM DTT, 10% glycerol, 1% Triton X-100, and a protease inhibitor mixture solution (Roche), for Western blot application. Human SPCA1a (Dode et al., 2005) was overexpressed in COS-1 and used as the control. Protein concentration was determined using the Lowry assay (Lowry et al., 1951).

*Western blot.* NuPAGE Bis-Tris Pre-Cast Gels (4–12%; Invitrogen) with 3-(*N*-morpholino)propanesulfonic acid running buffer were used for protein electrophoresis. Protein transfer to a polyvinylidene difluoride (PVDF) membrane was performed in a Mini Trans-Blot cell system (Bio-Rad). After blocking with Tris-buffered saline containing 0.1% Tween 20 (TBS-T) and 5% (w/v) nonfat dry milk for 1 h, the PVDF membrane was incubated for 3 h at room temperature with the following primary antibodies diluted in TBS containing 0.1% (v/v) Tween 20: anti-SPCA1 (1:4000) and anti-$\beta$ tubulin (1:8000). Next, the membrane was incubated with corresponding alkaline phosphatase-conjugated secondary antibodies (GE Healthcare) for 1 h at room temperature. The PVDF membranes were washed extensively with 0.5% milk in TBS-T between steps. The labeling was visualized by chemifluorescence using the ECF substrate (GE Healthcare) and scanned with the Storm scanner (GE Healthcare).

*Primary cultures of hippocampal neurons and DNA nucleofection.* Hippocampus was dissected from embryonic day 17 mouse embryos, collected in HBSS, and digested with 0.25% trypsin in HBSS for 15 min at 37°C. After gentle homogenization and rinsing in HBSS, dissociated hippocampal neurons were counted, and $4 \times 10^6$ cells were nucleofected with pSUPER-mouseSPCA1 using the Mouse Neuron Nucleofector kit (Amaxa Biosystems). Cotransfection with the pmaxGFP vector was used to identify transfected neurons. Then, the neurons were plated onto glass coverslips coated with 1 mg/ml poly-L-lysine in MEM containing 10% (v/v) horse serum and incubated at 37°C and 5% $CO_2$–95% air. After 3 h, the medium was replaced with Neurobasal medium supplemented with B27 and incubated for several days *in vitro*. Half of the culture medium was replaced with fresh medium once per week.

*Immunofluorescence.* N2a cells and hippocampal neurons seeded onto coverslips were washed with PBS and fixed with 4% paraformaldehyde in PBS for 20 min. Brains of adult Swiss mice (3 months old) were fixed by perfusion with the same fixative. Parasagittal cryostat sections were obtained as described by Sepúlveda et al. (2008). The

cells and the tissue sections were permeabilized with 0.2% Triton X-100 in PBS and blocked for 1 h with 3% BSA in PBS or 0.2% gelatin, 0.1 M lysine, and 0.25% Triton X-100 in PBS, respectively. The dual localization of proteins was done by incubating with a mixture of two primary antibodies diluted in the blocking solution for 2 h (anti-SPCA1, 1:500; GM130, 1:250; anti-$\beta$ tubulin, 1:1000; anti-SERCA2b, 1:500; or SMI312, 1:1000). Fluorescence labeling was obtained using the secondary antibodies Alexa594 goat anti-rabbit, Alexa488 goat anti-mouse, Alexa350 goat anti-mouse, or Alexa594 goat anti-mouse (1:500; Invitrogen) for 1 h. Staining with 10 $\mu$M 4′,6-diamidino-2-phenylindole (DAPI) was used to visualize nuclei. Then, the coverslips with cells and the slides with tissue sections were mounted with FluorSave medium and analyzed using an inverted Olympus IX81 fluorescence microscope. Negative controls were performed for every set of experiments by omitting the primary antibodies from the procedure.

*Analysis of morphology.* Six fields in every culture assay were chosen randomly and photographed. Determination of cell body diameter, body area, and neurite length were done with the NIH ImageJ program. N2a cells with one or more neurites of a length more than twice the body diameter were defined as differentiated (Cowley et al., 1994). An axon was considered significant in neurons if the length of the process was at least twice as long as any other process and was more than twice the cell body diameter, as described by Yin et al. (2008). The specified number and length of axons includes all axonal branches emerging from the main axon (distances from soma to tip of each axon branch).

*$Ca^{2+}$ imaging.* Cells in chamber slides were rinsed in Krebs' buffer (135 mM NaCl, 6 mM KCl, 1.2 mM $MgCl_2$, 12 mM glucose, 1.5 mM $CaCl_2$, 12 mM HEPES, pH 7.3), loaded with 2 $\mu$M Fura-2AM for 15 min at room temperature in darkness, and washed with Krebs' buffer for 15 min. Measurements were performed in $Ca^{2+}$-free solutions prepared by omitting $Ca^{2+}$ from the Krebs' buffer and including 2 mM EGTA. The viability of the cells was tested at the end of every experiment by the addition of Krebs' buffer. Cytosolic $Ca^{2+}$ was monitored during the assay on an inverted Olympus IX81 microscope equipped with a perfusion system at 37°C. Ratio measurements were performed every 4 s by excitation at 340 and 380 nm and recording of emission at 530 nm. The captured images were analyzed by Cell$^R$ software (Olympus). Ratio values were derived by averaging the fluorescence intensity from the entire cytosolic area.

*Quantification.* TINA software was used to quantify the intensity of the bands on the Western blots, and the ImageJ program was used to determine integrated density and maximum gray value of immunoreactions.

*Data analyses and statistics.* Data were processed and analyzed with the SigmaPlot software. Comparisons between two groups were

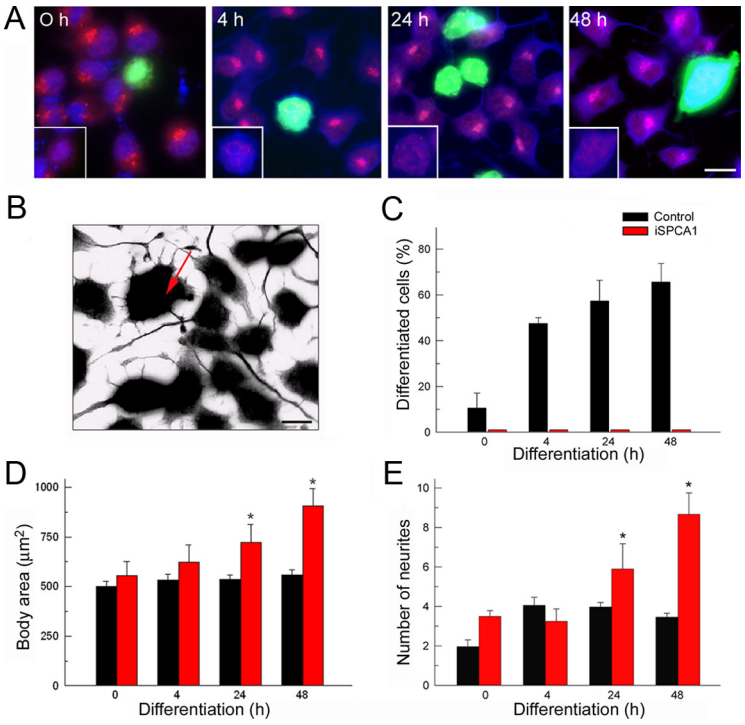


**Figure 2.** Effect of SPCA1 knockdown on the differentiation of N2a cells. ***A***, Double-immunofluorescence staining of SPCA1 (red) and $\beta$ tubulin (blue) at different stages of differentiation. GFP-positive transfected cells (green) were SPCA1 negative (insets). ***B***, Grayscale inverted image of $\beta$ tubulin immunoreaction as an example of the images used for quantification in ***C–E***. The arrow shows an SPCA1-interfered cell. ***C–E***, Effects of SPCA1 silencing on the percentage of differentiated cells (***C***), cell body area (***D***), and production of neurites (***E***), documenting suppression in differentiation. Data are mean ± SE from four preparations (*$p \leq 0.05$). Scale bars: ***A***, 27 $\mu$m; ***B***, 20 $\mu$m.

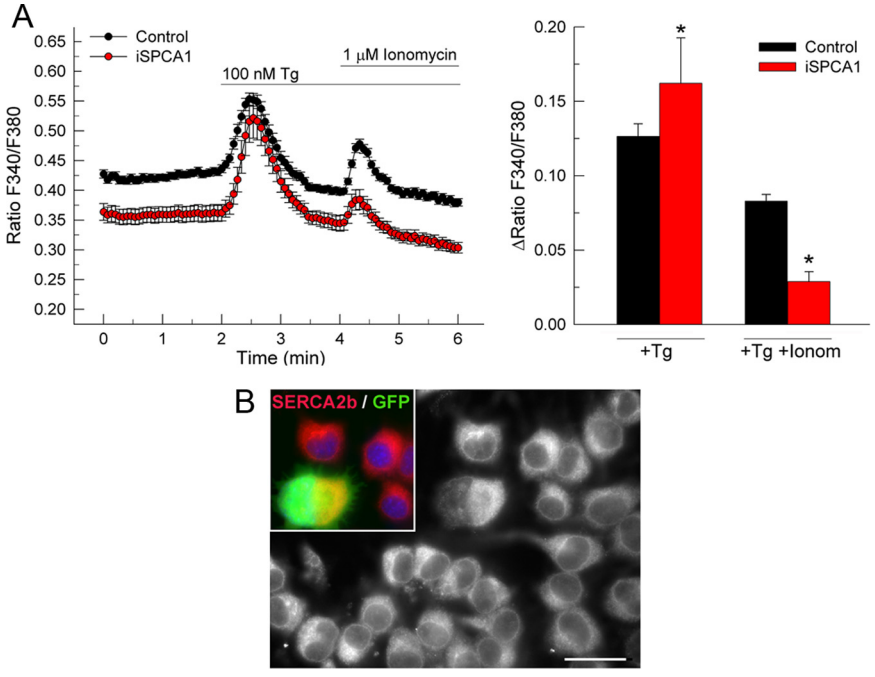


**Figure 3.** Effect of the silencing of SPCA1 expression on the Golgi $Ca^{2+}$ content in N2a cells. ***A***, $Ca^{2+}$ imaging assays in SPCA1-silenced N2a cells showing the Fura-2 fluorescence time course changes in $Ca^{2+}$-free medium. The top line indicates the incubation periods. The ratio of the Fura-2 fluorescence peak value of the release phase relative to preceding baseline is shown on the right. Data are mean ± SE of the response of ≥20 cells per experiment, performed in triplicate, from four preparations. ***B***, Immunofluorescence staining of anti-SERCA2b (red and gray) in N2a cell cultures transfected with pSUPER-mouse iSPCA1, where GFP-positive cells (green) are SPCA1 silenced. Nuclei were visualized with DAPI (blue). Semiquantification of SERCA2b-integrated density revealed a significant increase from 1.0 ± 0.04 arbitrary units (a.u.) in control cells to 1.65 ± 0.24 a.u. in SPCA1-interfered cells. No difference was observed after semiquantification of SERCA2b-maximum gray value in SPCA1-interfered cells (1.05 ± 0.02 a.u.) versus control cells (1.0 ± 0.02 a.u.). Data are mean ± SE of five experiments (*$p \leq 0.05$). Tg, Thapsigargin; Ionom, ionomycin. Scale bar, 37 $\mu$m.

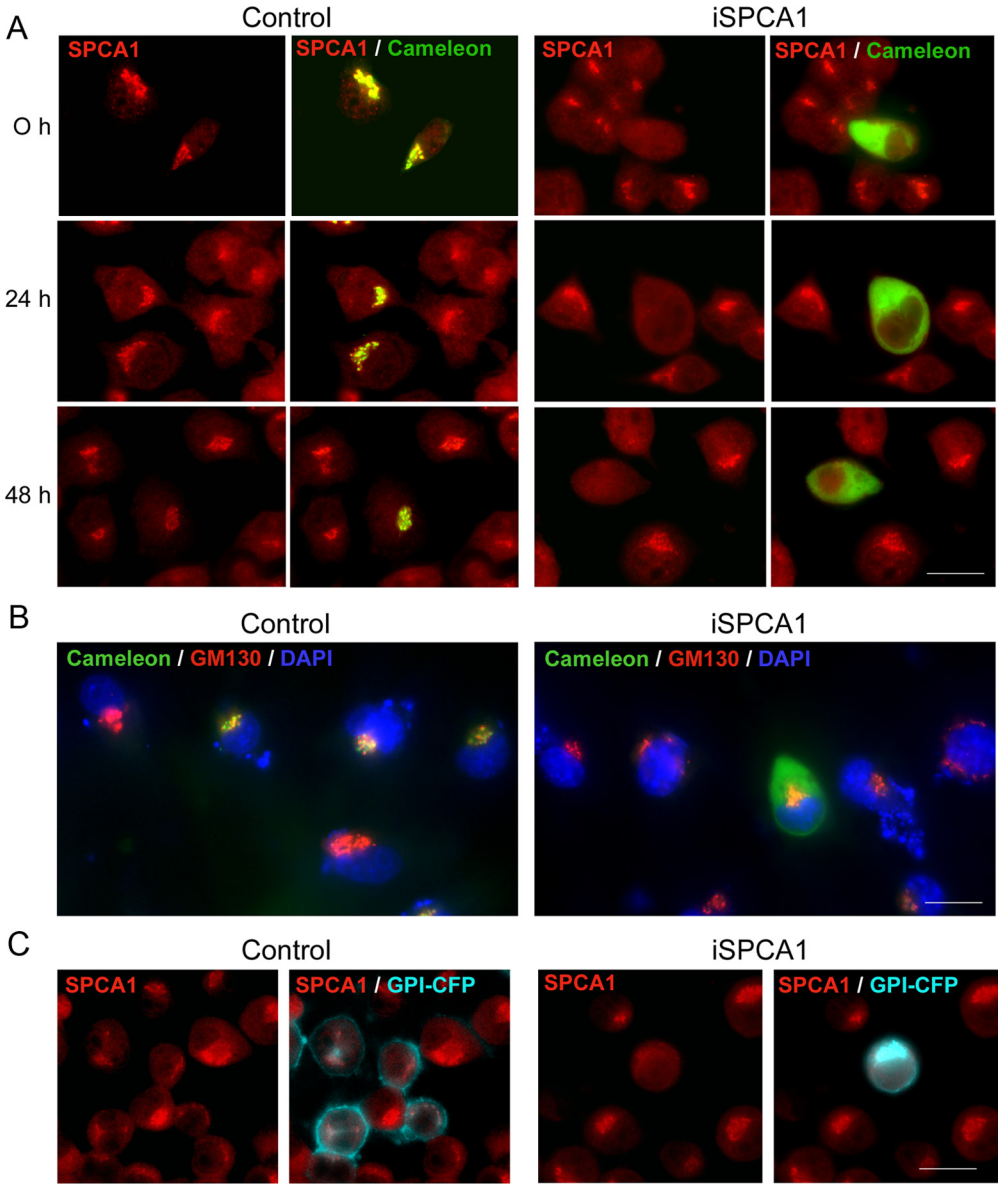


**Figure 4.** Effect of SPCA1 suppression on the localization of Golgi-cameleon in N2a cells. ***A***, Localization of SPCA1 (red) and Golgi-cameleon (green; colocalization in yellow) in control cells and in cells transfected with pSUPER-mouseSPCA1 (iSPCA1) and differentiated during 0, 24, and 48 h. Changes in the distribution of the cameleon protein is observed in SPCA1-suppressed cells. ***B***, Localization of the Golgi marker GM130 (red) and the Golgi-cameleon (green) in control and iSPCA1-N2a cell cultures after a 24 h differentiation. DAPI staining (blue) was used to visualize nuclei. ***C***, Distribution of SPCA1 (red) and CFP-GL-GPI (cyan) in control and SPCA1-interfered cells after 24 h of differentiation. The GPI construct is no longer targeted to the plasma membrane in iSPCA1 cells. Scale bars, 26 $\mu$m.

made using the unpaired Student's *t* test. Statistical significance was accepted when the *p* value was $\leq 0.05$.

## Results

### Knockdown of SPCA1 expression in N2a cells impairs neuronal differentiation

N2a cells can be differentiated to a neural cell type by incubation with retinoic acid (Gallo et al., 2002). This induced the production of neurites that can be clearly visualized after immunostaining with the anti-$\beta$ tubulin antibody (Fig. 1*A*). In these cells, SPCA1 was localized close to the nucleus in a single Golgi complex, where the Golgi marker GM130 was also present (Fig. 1*B*). To determine whether SPCA1 has a role in neuronal differentiation, we repressed the endogenous SPCA1 expression by transient transfection with the pSUPER-mouseSPCA1 vector. Analysis of cultures at 3 d after transfection revealed that transfected cells (i.e., GFP-positive cells) clearly lacked expression of SPCA1 protein (Fig. 1*C*). However, untransfected cells showed a juxtanuclear expression of SPCA1. FACS and Western blot analysis (Fig. 1*D*) revealed an efficient silencing of SPCA1 expression in the sorted GFP-positive cells.

In a subsequent step, we investigated the effect of SPCA1 silencing on neuronal differentiation. Cells were fixed at 0, 4, 24, and 48 h after induction of differentiation and double stained for immunofluorescence microscopy with SPCA1 and $\beta$ tubulin antibodies, to reveal, respectively, the suppression of the SPCA1 level and neurite production (Fig. 2*A*). Gray scale inverted images of $\beta$ tubulin immunoreactions (Fig. 2*B*) were used to quantify the total number of differentiated cells (containing at least one process greater than two cell body diameters in length) (Fig. 2*C*), the body diameter (Fig. 2*D*), and the number of neurites per

cell (Fig. 2*E*). Control cultures showed a gradual increase in the fraction of differentiated cells (Fig. 2*C*), whereas knockdown cells exhibited a total lack of differentiation. Remarkably, SPCA1-negative cells were larger than control cells (area covered by the cell body: control, 559.2 ± 24.3 $\mu m^2$; iSPCA1, 907.2 ± 85.8 $\mu m^2$ after 48 h of differentiation) (Fig. 2*D*); a larger cell size could thus indicate a lack of differentiation and/or compromised mitosis, since a structural change of the Golgi is an important checkpoint for mitosis (Colanzi et al., 2003; Colanzi and Corda, 2007). Furthermore, in control cells, the production of neurites was restricted to the first 4 h of differentiation (Fig. 2*E*) and was followed by a neurite elongation phase (data not shown). In contrast, in the SPCA1-suppressed cells, a very significant increase in the production of neurites was seen even after 24–48 h of incubation in differentiation medium (control, 3.46 ± 0.19; iSPCA1, 8.67 ± 1.08 at 48 h), but these processes were always of short length. These results thus show an important effect of SPCA1 suppression on neural differentiation.

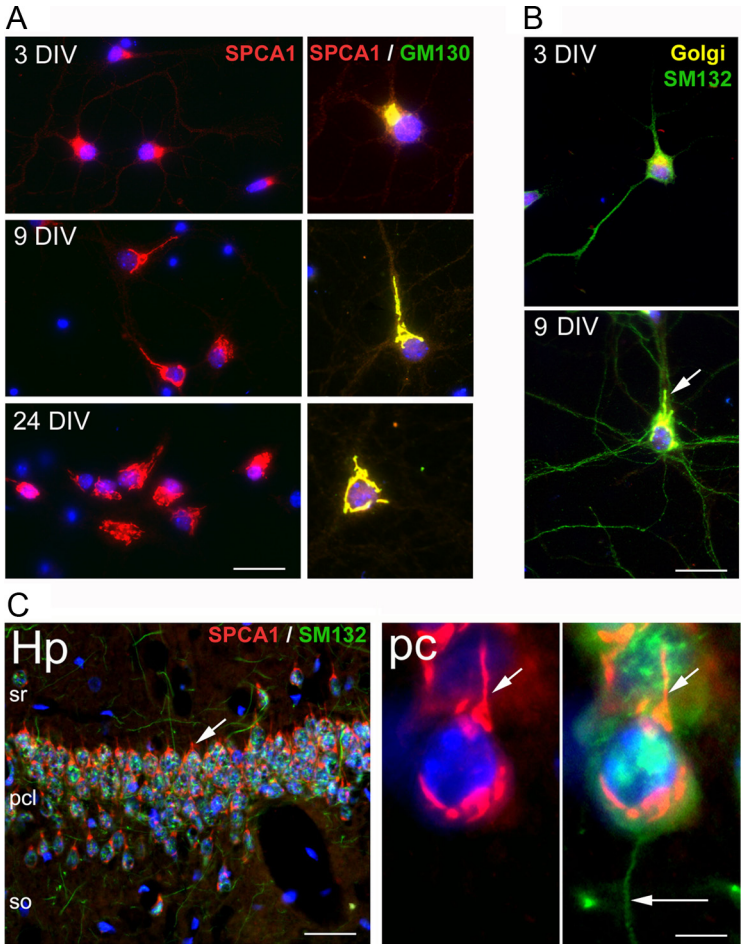


**Figure 5.** Localization of SPCA1 in cultured mouse hippocampal neurons and adult mouse hippocampus. ***A***, Double-immunofluorescence staining of SPCA1 (red) and the Golgi marker GM130 (green; colocalization in yellow) in neurons at the indicated DIV. Nuclei were visualized with DAPI staining (blue). ***B***, Immunodetection with the axon marker SMI312 (green) in neurons at 3 and 9 DIV. Golgi complexes are shown in yellow. The arrow indicates the apical dendritic trunk. ***C***, Distribution of SPCA1 (red) and SMI312 (green) in the CA3 region of the Amon's horn of 3-month-old mouse hippocampus. SPCA1 is expressed in Golgi stacks of the soma and primary dendritic trunks (short arrows) of the pyramidal neurons. However, axons (long arrow) are SPCA1 negative. Hp, Hippocampus; sr, stratum radiatus; pcl, pyramidal cell layer; so, stratum oriens; pc, hippocampal pyramidal cells. Scale bars: ***A***, 25 $\mu$m; ***B***, 15 $\mu$m; ***C***, 32 $\mu$m (inset, 9 $\mu$m).

### SPCA1 silencing alters $Ca^{2+}$ homeostasis in the Golgi of N2a cells

Cytosolic $Ca^{2+}$ signals were recorded in Fura-2AM-loaded cells, to analyze the effect of SPCA1 suppression on the Golgi and cytosolic $Ca^{2+}$ homeostasis (Fig. 3*A*). Basal cytosolic $Ca^{2+}$ concentration ($[Ca^{2+}]_c$) was measured in a $Ca^{2+}$-free medium. Of note, SPCA1-interfered cells showed a lower resting $[Ca^{2+}]_c$. The addition of 100 nM thapsigargin elicited a transient raise in $[Ca^{2+}]_c$ in control cells, as a result of the inhibition of the SERCA pump (Sagara et al., 1992), which leads to $Ca^{2+}$ depletion of the endoplasmic reticulum by an unopposed passive leak. After the basal $[Ca^{2+}]_c$ was stabilized, further addition of 1 $\mu$M ionomycin produced an increase in the $[Ca^{2+}]_c$, which is attributable to $Ca^{2+}$ release from stores that do not depend on SERCA activity. SPCA1-interfered cells showed a significant reduction (65%) of this $Ca^{2+}$ release after ionomycin addition, indicating the substantial contribution of the SPCA1-dependent Golgi stores to the SERCA-independent $Ca^{2+}$ pool. Interestingly, SPCA1-suppressed cells showed a higher rise in $[Ca^{2+}]_c$ after the first addition of thapsigargin compared with control cells. This could either reveal a compensatory upregulation of the specific amount or activity of SERCA pumps in the endoplasmic reticulum of these cells or merely indicate an increased endoplasmic reticulum volume. We therefore performed immunofluorescence with the SERCA2b antibody, directed against the major SERCA isoform in neural cells, followed by semiquantitative analysis (Fig. 3*B*). The SPCA1-interfered cells showed an increase (165%) of the SERCA2b-integrated density with respect to control cells. However, no difference was observed in the SERCA2b gray value per unit area, and hence the increase was entirely accounted by the increase in cell size (Fig. 2*D*) and consequently larger endoplasmic reticulum area.

### The silencing of SPCA1 in N2a cells alters the trafficking of the Golgi-localized cameleon and of a plasma membrane-localized GPI-anchored cyan fluorescent protein construct

To assess whether the impaired Golgi homeostasis resulting from SPCA1 suppression would affect protein trafficking in the secretory pathway in general or affect a specific class of Golgi resident proteins in transit, we first monitored the trafficking of a Golgi-targeted cameleon construct. This probe is targeted to the *medial/trans*-Golgi by the N-terminal region of galactosyltransferase (Griesbeck et al., 2001). Double transfections were done with the pSUPER-mouseSPCA1 vector and the Golgi-cameleon (13-fold molar excess of the pSUPER-mouseSPCA1 over Golgi-cameleon), and cells were analyzed at different stages of differentiation (Fig. 4). As expected, in control cells both SPCA1 and Golgi-cameleon colocalized in stacks of the Golgi complex, whereas in SPCA1-silenced cells the cameleon distribution was mainly observed in the cytosol (Fig. 4*A*). Conversely, GM130, a

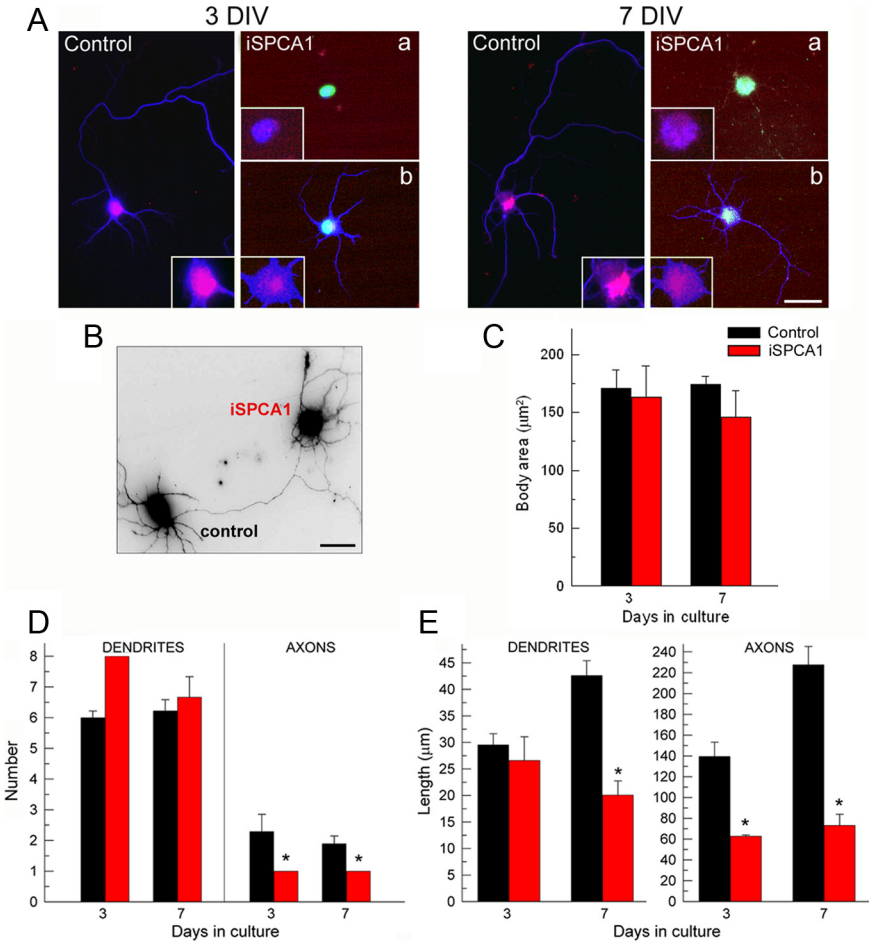


**Figure 6.** Effect of SPCA1 knockdown on primary hippocampal neurons. Neurons were nucleofected with the pSUPER empty vector (control) or the pSUPER-mouseSPCA1 (iSPCA1) to suppress SPCA1, seeded, and fixed at 3 and 7 DIV. ***A***, Double immunofluorescence with anti-SPCA1 (red) and anti-$\beta$ tubulin (blue). GFP-positive nucleofected cells (green) were classified in two populations: neurons with a total lack of neurite production (iSPCA1; ***a***) and cells with partial SPCA1-silencing showing an important delay in the differentiation (iSPCA1; ***b***). ***B–E***, Grayscale inverted image of $\beta$ tubulin immunoreaction representative of those used to quantify the body cell area (***C***) and the number (***D***) and length (***E***) of dendrites and axons at different DIV. Data are mean ± SE from three preparations (*$p \leq 0.05$). Scale bars: ***A***, 25 $\mu$m; ***B***, 15 $\mu$m.

matrix protein specifically attached to the cytosolic side of the *cis*-stacks of the Golgi complex, remained in its original localization in the SPCA1-silenced cells (Fig. 4*B*). We then assessed the effect of SPCA1 silencing on Golgi sorting steps known to be important for generating cellular polarity. N2a cells were therefore cotransfected with a GPI-anchored–cyan fluorescent protein (CFP) construct, a target that is also *N*-glycosylated (Keller et al., 2001). In control cells, the trafficking of this GPI-anchored construct follows its normal path from the *trans*-Golgi network structures to its final destination in the plasma membrane (Fig. 4*C*). In iSPCA1 cells however, the GPI construct was no longer targeted to the plasma membrane. Also the vesicular stomatitis virus–yellow fluorescent protein glycoprotein did not reach its destination in the plasma membrane upon SPCA1 knockdown but showed a vesicular distribution in the cytosol (results not shown).

### Suppression of SPCA1 in mouse hippocampal neurons also impairs neural polarity and $Ca^{2+}$ homeostasis in the Golgi

Primary cultures of mouse hippocampal neurons were also used since these represent a more physiological relevant context to study the impact of SPCA1 knockdown on $Ca^{2+}$ homeostasis and on the implementation of neural polarity. The cultured neurons followed the expected course of development as described previously (Dotti et al., 1988). The subcellular localization of SPCA1 in these cells was first analyzed by immunofluorescence assays at different days *in vitro* (DIV) (Fig. 5). SPCA1 was found to be highly expressed from the earliest stages in culture on, and it always colocalized with the Golgi marker GM130 (Fig. 5*A*). At 3 DIV, SPCA1 was located in the Golgi complex, which, at this stage of differentiation, forms a single-copy perinuclear organelle, as is also the case in N2a cells and in most of mammalian cells (Van Baelen et al., 2001; Wootton et al., 2004). However, at 9 DIV, the SPCA1 was found in multiple fragmented Golgi complexes that, at that stage, were spread over the entire soma but which showed a clear predominance in the apical dendritic trunk. The axon, which could be visualized with the marker SMI312, was devoid of SPCA1-positive complexes (Fig. 5*B*). A similar SPCA1 distribution was found in more mature neurons at 24 DIV. These results are comparable to those found in adult tissue (Fig. 5*C*) and also to those described in postnatal developing mouse hippocampal tissue (Sepúlveda et al., 2008).

SPCA1 silencing was then used to further analyze the role of SPCA1 in differentiation of hippocampal neurons. These cells were conucleofected with the pSUPER-mouseSPCA1 vector and GFP, seeded, and maintained in culture. After 3 d (required for the efficient knockdown) or 7 d, cells were immunostained for SPCA1 to assess the level of interference in the GFP-positive cells and for $\beta$ tubulin to determine the body cell area and the number and length of dendrites and axons (Fig. 6). Two populations of SPCA1-interfered neurons could be discriminated: one completely lacked SPCA1 expression, showed no neurites, and became apoptotic (Fig. 6*A*, top). In the other, SPCA1 was incompletely suppressed, and these cells showed a significant delay in differentiation (Fig. 6*A*, bottom). A detailed analysis of this second population was done at 3 and 7 DIV by measuring different parameters from gray scale inverted images of $\beta$ tubulin immunoreactions (Fig. 6*B*). Thus, a modest reduction in cell body area (Fig. 6*C*) for SPCA1-interfered neurons (145.9 ± 22 $\mu m^2$) with respect to control (174.4 ± 7 $\mu m^2$) was observed at 7 DIV. The number of dendrites (Fig. 6*D*) was not significantly different (control, 6.22 ± 0.36; iSPCA1, 6.67 ± 0.67), but the number of axonal branches (Fig. 6*D*) was considerably reduced (control, 1.89 ± 0.36; iSPCA1, 1 ± 0). Besides, dendrites and axons were much shorter in iSPCA1 cells than in control cells (Fig. 6*E*) (dendrites: control, 42.58 ± 2.81 $\mu$m; iSPCA1, 20.07 ± 2.67 $\mu$m; axons: control, 227.62 ± 17.6 $\mu$m; iSPCA1, 73.14 ± 10.7 $\mu$m).

$Ca^{2+}$-imaging assays with Fura-2AM were also performed to evaluate the functional impact of SPCA1 silencing on the $Ca^{2+}$ homeostasis of these neurons (Fig. 7). Like in N2a cells, resting $[Ca^{2+}]_c$ was lower in SPCA1-interfered cells. However, in con-

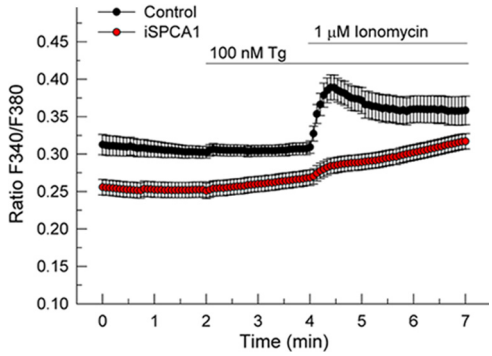


**Figure 7.** Effect of the silencing of SPCA1 on $Ca^{2+}$ content of the Golgi stores in hippocampal neurons. $Ca^{2+}$-imaging assays of neurons in primary culture loaded with Fura-2AM. The experiment was performed in a $Ca^{2+}$-free medium. The top line indicates the incubation periods. The ratio of the Fura-2 fluorescence peak after ionomycin addition relative to baseline showed a significant decrease from 0.082 ± 0.011 in control cells to 0.022 ± 0.003 in SPCA1-interfered neurons. Data are mean ± SE of the response of seven or more neurons per experiment, performed in triplicate, from three preparations ( $p \leq 0.05$). Tg, Thapsigargin.

trast to what is seen in N2a cells, the addition of 100 nM thapsigargin did not evoke a significant transient $Ca^{2+}$ release. This is consistent with previous reports showing that baseline endoplasmic reticulum $Ca^{2+}$ content in hippocampal neurons is very low in these assay conditions (Irving and Collingridge, 1998; Baba et al., 2003). Similar to N2a cells, further addition of ionomycin produced a fast $Ca^{2+}$ release into the cytosol in control cells, whereas the SPCA1-interfered neurons showed a significant reduction (76%) in this SERCA-independent, presumably mainly Golgi-derived $Ca^{2+}$ release (Fig. 7). The slow rise of cytosolic $Ca^{2+}$ in SPCA1-interfered cells could represent release from acidic non-Golgi stores such as lysosomes, since the action of ionomycin on these stores is known to be inefficient. In contrast, in control cells the later phase of the ionomycin effect could be dominated by $Ca^{2+}$ extrusion across the plasma membrane, explaining the slow decline of the signal after the large and fast, presumably Golgi-derived $Ca^{2+}$ release.

## Discussion

This study reveals a role of the Golgi-based SPCA1 pump in helping to establish neural polarity. The knock down of SPCA1 expression by means of short interfering RNA in the N2a cell line and in hippocampal cultured neurons disrupts polarized membrane trafficking and results in the generation of an aberrant number of abnormally short neurites. Such an impaired neural polarity would critically affect the normal function of the nervous system. Dendrites and axons differ in morphology, molecular composition, and synaptic polarity (Bartlett and Banker, 1984a,b), which results in different functional properties. It has been reported that the *trans*-Golgi network plays a pivotal role in this morphological polarization (Tang, 2001; Horton et al., 2005). We now documented spatial–temporal changes in SPCA1 localization reflecting such reorganization in hippocampal neurons. The SPCA1 distribution shifts from one corresponding to a single-copy juxtanuclear Golgi position to multiple complexes distributed over the neural soma, with a clear preference for dendritic positioning in stages of rapid dendritic outgrowth (Horton and Ehlers, 2003). This *in vitro* pattern is similar to that observed in mouse developing brain (Sepúlveda et al., 2008). In fact, it has been recently reported that growth of neuronal dendrites is more dependent on the classical secretory pathway than axon growth, a property that is probably related to the position of the somatic Golgi toward the dendrites (Horton and Ehlers, 2003; Ye et al., 2007). This suggests a specific function of the Golgi in organizing a directed flow of secretory traffic.

Morphological rearrangement of Golgi positioning, as shown during neural development, is also accompanying other cellular events such as cell division and apoptosis. Perinuclear Golgi fragmentation is a prerequisite, and indeed its occurrence represents an important checkpoint for mitosis (Colanzi et al., 2003; Colanzi and Corda, 2007). Similarly, in response to apoptotic stimuli, the Golgi apparatus breaks down into small vesiculotubular elements (Sesso et al., 1999). Golgi fragmentation seems to be involved in early and probably irreversible cellular reorganizations leading to neurodegenerative diseases such as amyotrophic lateral sclerosis, Alzheimer's disease, and Creutzfeldt-Jacob disease (Gonatas et al., 2006). In both physiological and pathological conditions, fragmentation involves posttranslational modification and reorganization of Golgi proteins (Dirac-Svejstrup et al., 2000; Allan et al., 2002; Lane et al., 2002). Our results suggest that similar signaling cascades may also operate in the neuronal setting to regulate Golgi distribution during development. Furthermore, changes in SPCA expression have been observed in rats after ischemic preconditioning, an adaptation event that results in increased protection of the brain to severe ischemia (Pavlíková et al., 2009).

Since SPCA1 can also transport $Mn^{2+}$, the alteration of neural polarity after silencing of SPCA1 is expected to result from a deficiency of $Ca^{2+}$ and/or $Mn^{2+}$ uptake into the Golgi store, and the subsequent reduction of its $Ca^{2+}$ and/or $Mn^{2+}$ content, as was the case of $Ca^{2+}$, documented by our $Ca^{2+}$-imaging assays. $Ca^{2+}$ and $Mn^{2+}$ are critical cofactors in many Golgi activities, which include the correct processing and trafficking of newly synthesized proteins and membranes required for neural polarity. Proteins such as glycosyltransferases (Roseman, 2001), sulfotransferases (Mishiro et al., 2004; Seko et al., 2005), and prohormone convertases (Anderson et al., 1997; LaFerla, 2002) need $Ca^{2+}$ and/or $Mn^{2+}$ for their activity. In fact, downregulation of SPCAs interferes with glycosylation of thyroglobulin in rat thyrocytes (Ramos-Castaneda et al., 2005). In contrast, our results on N2a cells suggest that disturbed $Ca^{2+}$ handling by the Golgi function could partly be compensated by the endoplasmic reticulum. SPCA1-interfered N2a cells are larger and therefore contain more endoplasmic reticulum. There is, however, no change in the amount of SERCA per unit membrane surface in the reticulum.

Hippocampal neurons were very vulnerable to $Ca^{2+}$ homeostasis disruption by SPCA1 silencing. This is in line with the observation that SPCA1 knock-out mice exhibit embryonic growth retardation with, in particular, malformations in the neural tube and that they do not survive beyond gestation day 10.5 (Okunade et al., 2007). Besides, Golgi membranes of Spca1(−/−) embryos were dilated, the number of Golgi-associated vesicles was augmented, and a large increase in cytoplasmic lipid was observed, consistent with impaired handling of lipids by the Golgi. Although in our study GM130, a matrix protein involved in maintaining the *cis*-Golgi structure (Nakamura et al., 1995), is not affected in SPCA1-interfered N2a cells, the *trans*-Golgi reporter cameleon (i.e., a protein protruding into the Golgi lumen and anchored in the membrane of the *trans*-Golgi by means of an N-terminal transmembrane segment of galactosyltransferase) and CFP-GL-GPI (i.e., a GPI-anchored reporter protein) were dramatically mislocalized. That reflects the importance of the Golgi in these trafficking processes.

Recent reports describe dendritic Golgi outposts as novel and additional components of the neural secretory pathway that control process outgrowth during early periods of neuronal differentiation (Horton and Ehlers, 2003; Tang, 2008). We could not immunodetect SPCA1 in these Golgi outposts of dendrites. In branches of the dendrites (Horton and Ehlers, 2003) and even in the dendritic spines (Spacek and Harris, 1997), the endoplasmic reticulum has been reported to represent an important $Ca^{2+}$ regulatory store. Therefore, the role of SPCA1 could be confined to a more general control of the secretory pathway in the Golgi apparatus. Neuronal SPCA1 expression is indispensable since total suppression in hippocampal neurons leads to apoptosis.

The formation and maintenance of somatodendritic and axonal plasma membrane domains requires a specific spatiotemporal regulation to which SPCA1 might contribute. This opens new fields for additional exploration of specific functions of SPCA in the secretory pathway.

## References


Allan VJ, Thompson HM, McNiven MA (2002) Motoring around the Golgi. Nat Cell Biol 4:E236–E242.

Anderson ED, VanSlyke JK, Thulin CD, Jean F, Thomas G (1997) Activation of the furin endoprotease is a multiple-step process: requirements for acidification and internal propeptide cleavage. EMBO J 16:1508–1518.

Baba A, Yasui T, Fujisawa S, Yamada RX, Yamada MK, Nishiyama N, Matsuki N, Ikegaya Y (2003) Activity-evoked capacitative $Ca^{2+}$ entry: implications in synaptic plasticity. J Neurosci 23:7737–7741.

Bartlett WP, Banker GA (1984a) An electron microscopic study of the development of axons and dendrites by hippocampal neurons in culture. I. Cells which develop without intercellular contacts. J Neurosci 4:1944–1953.

Bartlett WP, Banker GA (1984b) An electron microscopic study of the development of axons and dendrites by hippocampal neurons in culture. II. Synaptic relationships. J Neurosci 4:1954–1965.

Chua CE, Tang BL (2008) Syntaxin 16 is enriched in neuronal dendrites and may have a role in neurite outgrowth. Mol Membr Biol 25:35–45.

Colanzi A, Corda D (2007) Mitosis controls the Golgi and the Golgi controls mitosis. Curr Opin Cell Biol 19:386–393.

Colanzi A, Suetterlin C, Malhotra V (2003) Cell-cycle-specific Golgi fragmentation: how and why? Curr Opin Cell Biol 15:462–467.

Cowley S, Paterson H, Kemp P, Marshall CJ (1994) Activation of MAP kinase kinase is necessary and sufficient for PC12 differentiation and for transformation of NIH 3T3 cells. Cell 77:841–852.

Dirac-Svejstrup AB, Shorter J, Waters MG, Warren G (2000) Phosphorylation of the vesicle-tethering protein p115 by a casein kinase II-like enzyme is required for Golgi reassembly from isolated mitotic fragments. J Cell Biol 150:475–488.

Dode L, Andersen JP, Raeymaekers L, Missiaen L, Vilsen B, Wuytack F (2005) Functional comparison between secretory pathway $Ca^{2+}/Mn^{2+}$-ATPase (SPCA) 1 and sarcoplasmic reticulum Ca2+-ATPase (SERCA) 1 isoforms by steady-state and transient kinetic analyses. J Biol Chem 280:39124–39134.

Dotti CG, Sullivan CA, Banker GA (1988) The establishment of polarity by hippocampal neurons in culture. J Neurosci 8:1454–1468.

Gallo R, Zazzeroni F, Alesse E, Mincione C, Borello U, Buanne P, D'Eugenio R, Mackay AR, Argenti B, Gradini R, Russo MA, Maroder M, Cossu G, Frati L, Screpanti I, Gulino A (2002) REN: a novel, developmentally regulated gene that promotes neural cell differentiation. J Cell Biol 158:731–740.

Gonatas NK, Stieber A, Gonatas JO (2006) Fragmentation of the Golgi apparatus in neurodegenerative diseases and cell death. J Neurol Sci 246:21–30.

Griesbeck O, Baird GS, Campbell RE, Zacharias DA, Tsien RY (2001) Reducing the environmental sensitivity of yellow fluorescent protein. Mechanism and applications. J Biol Chem 276:29188–29194.

Horton AC, Ehlers MD (2003) Dual modes of endoplasmic reticulum-to-Golgi transport in dendrites revealed by live-cell imaging. J Neurosci 23:6188–6199.

Horton AC, Racz B, Monson EE, Lin AL, Weinberg RJ, Ehlers MD (2005) Polarized secretory trafficking directs cargo for asymmetric dendrite growth and morphogenesis. Neuron 48:757–771.

Irving AJ, Collingridge GL (1998) A characterization of muscarinic receptor-mediated intracellular $Ca^{2+}$ mobilization in cultured rat hippocampal neurones. J Physiol 511:747–759.

Keller P, Toomre D, Diaz E, White J, Simons K (2001) Multicolour imaging of post-Golgi sorting and trafficking in live cells. Nat Cell Biol 3:140–149.

LaFerla FM (2002) Calcium dyshomeostasis and intracellular signalling in Alzheimer's disease. Nat Rev Neurosci 3:862–872.

Lane JD, Lucocq J, Pryde J, Barr FA, Woodman PG, Allan VJ, Lowe M (2002) Caspase-mediated cleavage of the stacking protein GRASP65 is required for Golgi fragmentation during apoptosis. J Cell Biol 156:495–509.

Lowry OH, Rosebrough NJ, Farr AL, Randall RJ (1951) Protein measurement with the Folin phenol reagent. J Biol Chem 193:265–275.

Mata AM, Sepúlveda MR (2005) Calcium pumps in the central nervous system. Brain Res Brain Res Rev 49:398–405.

Mishiro E, Liu MY, Sakakibara Y, Suiko M, Liu MC (2004) Zebrafish tyrosylprotein sulfotransferase: molecular cloning, expression, and functional characterization. Biochem Cell Biol 82:295–303.

Murin R, Verleysdonk S, Raeymaekers L, Kaplan P, Lehotsky J (2006) Distribution of secretory pathway $Ca^{2+}$ ATPase (SPCA1) in neuronal and glial cell cultures. Cell Mol Neurobiol 26:1355–1365.

Nakamura N, Rabouille C, Watson R, Nilsson T, Hui N, Slusarewicz P, Kreis TE, Warren G (1995) Characterization of a cis-Golgi matrix protein, GM130. J Cell Biol 131:1715–1726.

Okunade GW, Miller ML, Azhar M, Andringa A, Sanford LP, Doetschman T, Prasad V, Shull GE (2007) Loss of the Atp2c1 secretory pathway $Ca^{2+}$-ATPase (SPCA1) in mice causes Golgi stress, apoptosis, and midgestational death in homozygous embryos and squamous cell tumors in adult heterozygotes. J Biol Chem 282:26517–26527.

Pavlíková M, Tatarkova Z, Sivonova M, Kaplan P, Krizanova O, Lehotsky J (2009) Alterations induced by ischemic preconditioning on secretory pathways $Ca^{2+}$-ATPase (SPCA) gene expression and oxidative damage after global cerebral ischemia/reperfusion in rats. Cell Mol Neurobiol 29:909–916.

Ramos-Castaneda J, Park YN, Liu M, Hauser K, Rudolph H, Shull GE, Jonkman MF, Mori K, Ikeda S, Ogawa H, Arvan P (2005) Deficiency of ATP2C1, a Golgi ion pump, induces secretory pathway defects in endoplasmic reticulum (ER)-associated degradation and sensitivity to ER stress. J Biol Chem 280:9467–9473.

Roseman S (2001) Reflections on glycobiology. J Biol Chem 276: 41527–41542.

Sagara Y, Fernandez-Belda F, de Meis L, Inesi G (1992) Characterization of the inhibition of intracellular $Ca^{2+}$ transport ATPases by thapsigargin. J Biol Chem 267:12606–12613.

Seko A, Sumiya J, Yamashita K (2005) Porcine, mouse and human galactose 3-O-sulphotransferase-2 enzymes have different substrate specificities; the porcine enzyme requires basic compounds for its catalytic activity. Biochem J 391:77–85.

Sepúlveda MR, Berrocal M, Marcos D, Wuytack F, Mata AM (2007) Functional and immunocytochemical evidence for the expression and localization of the secretory pathway $Ca^{2+}$-ATPase isoform 1 (SPCA1) in cerebellum relative to other $Ca^{2+}$ pumps. J Neurochem 103:1009–1018.

Sepúlveda MR, Marcos D, Berrocal M, Raeymaekers L, Mata AM, Wuytack F (2008) Activity and localization of the secretory pathway $Ca^{2+}$-ATPase isoform 1 (SPCA1) in different areas of the mouse brain during postnatal development. Mol Cell Neurosci 38:461–473.

Sesso A, Fujiwara DT, Jaeger M, Jaeger R, Li TC, Monteiro MM, Correa H, Ferreira MA, Schumacher RI, Belisario J, Kachar B, Chen EJ (1999) Structural elements common to mitosis and apoptosis. Tissue Cell 31:357–371.

Spacek J, Harris KM (1997) Three-dimensional organization of smooth endoplasmic reticulum in hippocampal CA1 dendrites and dendritic spines of the immature and mature rat. J Neurosci 17:190–203.

Sytnyk V, Leshchyns'ka I, Dityatev A, Schachner M (2004) Trans-Golgi network delivery of synaptic proteins in synaptogenesis. J Cell Sci 117:381–388.

Tang BL (2001) Protein trafficking mechanisms associated with neurite outgrowth and polarized sorting in neurons. J Neurochem 79:923–930.

Tang BL (2008) Emerging aspects of membrane traffic in neuronal dendrite growth. Biochim Biophys Acta 1783:169–176.

Ton VK, Mandal D, Vahadji C, Rao R (2002) Functional expression in yeast of the human secretory pathway $Ca^{2+}$, $Mn^{2+}$-ATPase defective in Hailey-Hailey disease. J Biol Chem 277:6422–6427.

Van Baelen K, Vanoevelen J, Missiaen L, Raeymaekers L, Wuytack F (2001) The Golgi PMR1 P-type ATPase of *Caenorhabditis elegans*. Identification of the gene and demonstration of calcium and manganese transport. J Biol Chem 276:10683–10691.

Van Baelen K, Vanoevelen J, Callewaert G, Parys JB, De Smedt H, Raeymaekers L, Rizzuto R, Missiaen L, Wuytack F (2003) The contribution of the SPCA1 $Ca^{2+}$ pump to the $Ca^{2+}$ accumulation in the Golgi apparatus of HeLa cells assessed via RNA-mediated interference. Biochem Biophys Res Commun 306:430–436.

Vanoevelen J, Dode L, Van Baelen K, Fairclough RJ, Missiaen L, Raeymaekers L, Wuytack F (2005) The secretory pathway $Ca^{2+}$/$Mn^{2+}$-ATPase 2 is a Golgi-localized pump with high affinity for $Ca^{2+}$ ions. J Biol Chem 280:22800–22808.

Wootton LL, Argent CC, Wheatley M, Michelangeli F (2004) The expression, activity and localisation of the secretory pathway $Ca^{2+}$-ATPase (SPCA1) in different mammalian tissues. Biochim Biophys Acta 1664:189–197.

Wuytack F, Eggermont JA, Raeymaekers L, Plessers L, Casteels R (1989) Antibodies against the non-muscle isoform of the endoplasmic reticulum $Ca^{2+}$-transport ATPase. Biochem J 264:765–769.

Xiang M, Mohamalawari D, Rao R (2005) A novel isoform of the secretory pathway $Ca^{2+}$,$Mn^{2+}$-ATPase, hSPCA2, has unusual properties and is expressed in the brain. J Biol Chem 280:11608–11614.

Ye B, Zhang Y, Song W, Younger SH, Jan LY, Jan YN (2007) Growing dendrites and axons differ in their reliance on the secretory pathway. Cell 130:717–729.

Yin DM, Huang YH, Zhu YB, Wang Y (2008) Both the establishment and maintenance of neuronal polarity require the activity of protein kinase D in the Golgi apparatus. J Neurosci 28:8832–8843.